

# Molecular Motion of the PMMA Chain in Poly(methyl methacrylate)/Poly(vinylidene fluoride) Blends by Spin Trapping Labeling

Shigetaka Shimada,\* Yasurō Hori, and Hisatsugu Kashiwabara

Nagoya Institute of Technology, Gokiso-cho, Showa-ku, Nagoya 466, Japan.  
Received August 12, 1987

**ABSTRACT:** Spin trapping is used to study molecular motion of PMMA chains in blends of poly(methyl methacrylate)/poly(vinylidene fluoride) (PMMA/PVDF). Free radicals produced by thermal degradation of PMMA chains in the blends are trapped by 2,4,6-tri-*tert*-butylnitrosobenzene, and the spin-labeled chain ends are studied by electron spin resonance (ESR). The temperature dependence of the ESR spectra changes substantially as a function of the PVDF content of the blend. The narrowing curve of the outermost splitting widths and the generation curve of the mobile fraction of the spin label shift to low temperatures with increasing PVDF content of the blend. The decay of the spin label follows second-order kinetics, and the rate constant increases with increasing PVDF content of the blend. The decay reactions are interpreted in terms of a bimolecular reaction of the spin label and translational diffusion of the PMMA chains. These phenomena indicate that the rotational and translational molecular motions of the PMMA chains are closely related to the compatibility of the PMMA and PVDF in the noncrystalline region of the blends.

## Introduction

Many workers have studied blends of poly(methyl methacrylate) (PMMA) and poly(vinylidene fluoride) (PVDF) by such techniques as differential scanning calorimetry, X-ray diffraction, light scattering, dynamic mechanical, and dielectric measurements.<sup>1</sup> However, there are few studies by electron spin resonance (ESR). We have developed spin-label techniques<sup>2-4</sup> to investigate the structure and dynamic behavior of polymer chains at a particular site. ESR is a simple and effective method for determining molecular compatibility and molecular motion of a particular polymer chain in a blend. Blends of PMMA and PVDF generally have a complicated structure composed of a crystalline phase of PVDF and a liquidlike amorphous phase of PMMA/PVDF. The latter phase may include both PMMA-rich and PVDF-rich regions in a phase-separated system.

When PMMA and PVDF are completely compatible, the amorphous phase has only one region. Hirata and Kotaka<sup>1b</sup> concluded that phase separation occurs in a melt of PMMA and PVDF and that quenching the melt leads to a four-phase morphology. They used dynamic mechanical measurements to study the glass-rubber transition of the amorphous mixture and the crystallization and remelting of a PVDF crystalline phase. On the other hand, Hahn et al.<sup>1a</sup> concluded from dielectric relaxation data that the  $\beta$  transition of PVDF arises in the crystal-amorphous interface, where PMMA is completely excluded. However, the transitions of semicrystalline blends observed by mechanical and dielectric measurements are complicated because they include many relaxations involving the two polymer components and more than two phases, and it is difficult to separate the weak lower transitions from more intense and broad peaks. We here present the results of a spin-label study of the molecular relaxation of PMMA chains in PMMA/PVDF blends.

## Experimental Section

**Materials.** Powders of PVDF (Kynar 731) and PMMA (medium molecular weight) were from Pen-Walt Chemical Co. and Aldrich Chemical Co., respectively.

**Preparation of Blends.** Mixtures of PMMA and PVDF powders in ratios of 33:67 and 11:89 (w/w) and ~0.1% (w) of the spin trapping reagent 2,4,6-tri-*tert*-butylnitrosobenzene were dissolved in acetone at 50 °C. Films were prepared by casting from ~3% (w) of acetone solution at 50 °C. The blends were coded 33/67 and 11/89. Films of PMMA and PVDF containing the spin-trapping reagent were prepared by the same method.

**ESR Measurements.** Polymer samples were put into ESR sample tubes, evacuated to  $10^{-6}$  Torr, and thermally degraded. ESR measurements were carried out with a JEOL ME-3X X-band spectrometer with 100-kHz modulation. Spectra were recorded with a MELCOM 70/25 computer connected to the spectrometer. The signal of diphenylpicrylhydrazyl (DPPH) was used as a *g* value standard. The magnetic field sweep was calibrated with the splitting constant of  $\text{Mn}^{2+}$ .

## Results and Discussion

**ESR Spectra of Spin Adducts Labeled to PMMA Chains in Thermally Degraded Blends.** The thermal degradation of PMMA and polyethylene produces free radicals that can be trapped by a spin-trapping reagent and observed by ESR.<sup>3,5</sup> Figure 1 shows examples of the ESR spectra of the spin adducts trapped in PMMA after annealing at 173 °C for 15 min. For identification of the stable radicals, 0.2 g of the spin-labeled PMMA was dissolved in 0.5 mL of benzene under vacuum. The ESR spectrum of the benzene solution has considerable hyperfine structure (Figure 2). The hyperfine coupling constants due to the interaction with the nitrogen nucleus ( $a_N$ ) and meta protons in the benzene ring ( $a_H$ ) were  $0.959 \pm 0.009$  and  $0.189 \pm 0.004$  mT, respectively, and the *g* value was 2.00394. These values agree well with data obtained by Terabe and Konaka<sup>6</sup> for the anilino radical in benzene solution, which are  $a_N = 1.001$ – $1.101$  mT,  $a_H = 0.179$ – $0.207$  mT, and *g* = 2.0036–2.0040. Hence the stably trapped radicals can be considered to be as shown:

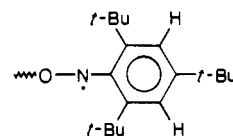
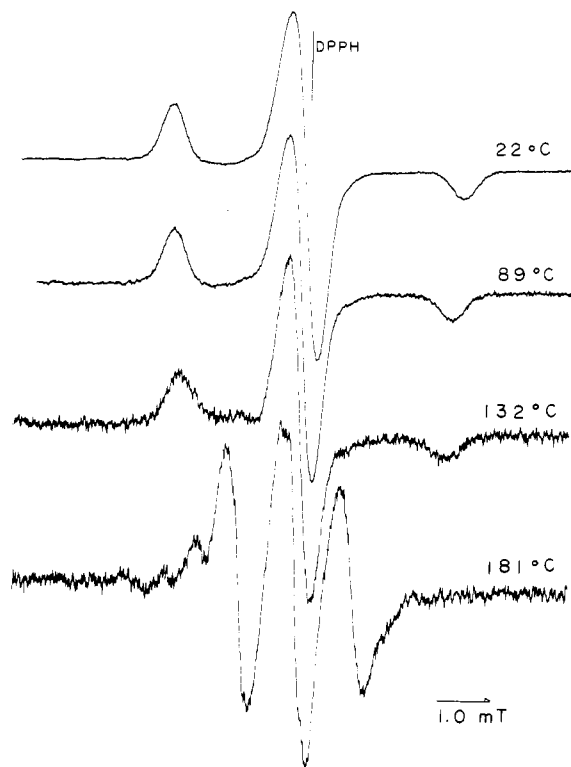


Figure 3 shows the concentration of the stable radicals as a function of annealing temperature. A sample containing the spin-trapping reagent was annealed at elevated temperature for 15 min and then plunged into liquid nitrogen, and ESR measurements were carried out at -196 °C. The concentrations of the radicals were obtained by double integration of the first derivative patterns. The generation curve shown in Figure 3 was obtained by repeating this procedure at increasing annealing temperatures.

In PMMA, radicals started to generate at ~120 °C and show a peak concentration around 176 °C, whereas only a small amount of radicals was produced from PVDF. In the 33/67 and 11/89 blends, the amount of radical species was proportional to the weight percent of PMMA in the





**Figure 4.** ESR spectra of spin labels (anilino radicals) in PMMA/PVDF (33/67) blend at various temperatures. The spectrum of DPPH,  $g = 2.0036$ , is the vertical line.

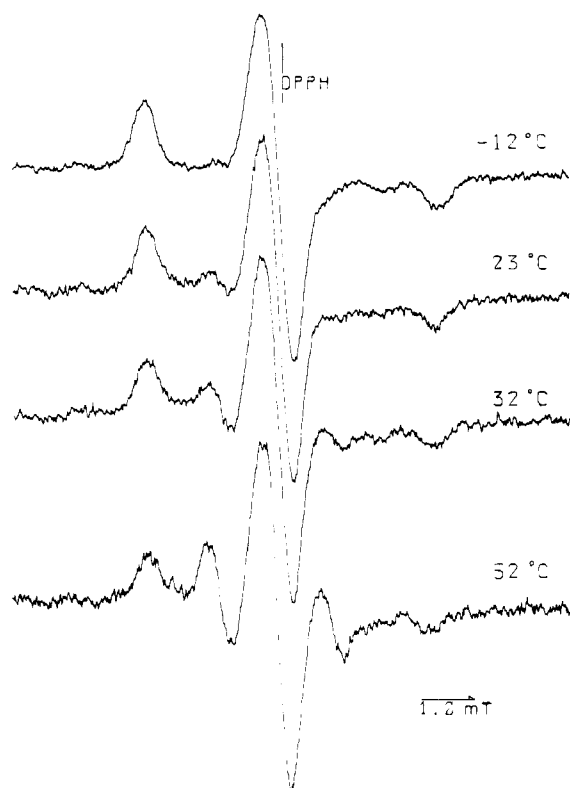


**Figure 5.** ESR spectra of spin labels (anilino radicals) in PMMA/PVDF (11/89) blend at various temperatures. The spectrum of DPPH,  $g = 2.0036$ , is the vertical line.

were measured at various temperatures. The widths narrowed with increasing temperature because of averaging of the anisotropic hyperfine coupling due to rotational motion of PMMA chains. In PMMA, the outermost peaks gradually changed around 60 °C and narrowed sharply at 160 °C (Figure 7). On the other hand, in the blends the

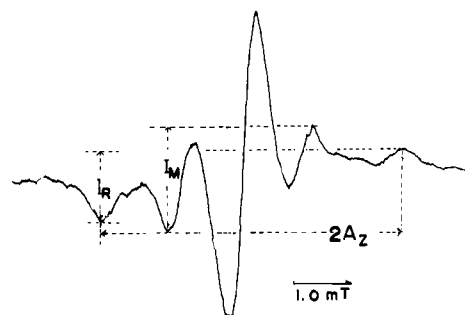


**Figure 6.** Example of an ESR spectrum composed of two spectra arising from spin labels with different mobilities. The relative intensities of the two spectra ( $I_M/I_R$ ) and extrema separation ( $2A_z$ ) are indicated.

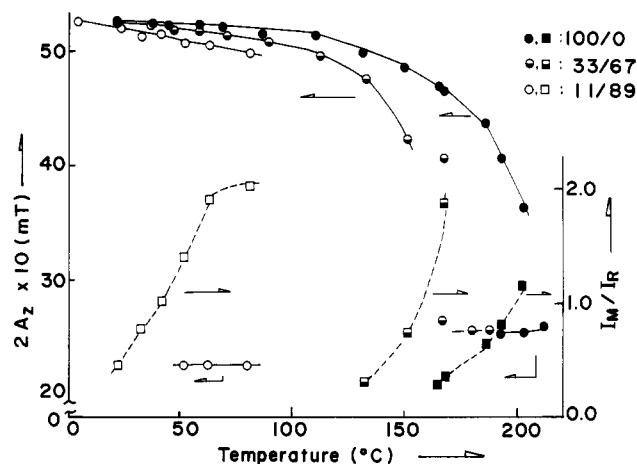


**Figure 7.** Variation of extrema separation ( $2A_z$ ) and mobility ratio ( $I_M/I_R$ ) with temperature: PMMA (●, ■); PMMA/PVDF blend (33/67) (○, □); PMMA/PVDF blend (11/89) (○, □). At higher temperatures, the values of  $2A_z$  of narrow components are also plotted.

narrowing curves shifted to lower temperatures with increasing content of PVDF; data could not be obtained in the high-temperature region.

The outermost splitting width of the narrow component ( $\sim 2.3$  mT) is independent of temperature (Figure 7). The positions of the outermost peaks coincide with those of the spectrum obtained with complete averaging of the anisotropic hyperfine splitting, as observed by Murakami and Sohma.<sup>7</sup> Hence we conclude that our ESR spectra are composed of two spectra arising from anilino radicals with different mobilities and that the narrow component arises from the spin label in a liquidlike state.<sup>7</sup> Since segmental mobility and relaxation processes reflect the free volume, the two spectral components must be associated with the free volume. In general, polymer chains have a broad distribution of relaxation times. As a result, immobile components should convert to mobile components, i.e., a liquidlike state, gradually with increasing temperature.

The ratios of mobile to immobile components,  $I_M/I_R$ , are shown in Figure 6 and plotted in Figure 7. The value of  $I_M/I_R$ , which is a crude measure of the mobile fraction of the spin-labeled PMMA chain, the guest polymer, increases with temperature. It is interesting that this plot of  $I_M/I_R$  shifts to lower temperatures with increasing content of PVDF in the blends. This result indicates an increase in the segmental mobility of the host polymer in the blends, reflecting the excess volume generated by molecular compatibility of PMMA and PVDF.

These temperature dependences indicate that the relaxations of PMMA chains in both mobile and immobile phases of the blends become rapid with increasing mo-

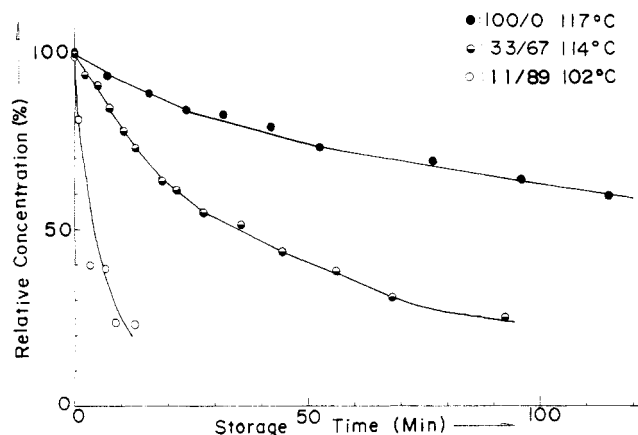


**Figure 8.** Decay curve of anilino radicals trapped in PMMA (●), PMMA/PVDF (33/67) blend (◐), and PMMA/PVDF (11/89) blend (○). Experiments were made at 117, 114, and 102 °C, respectively.

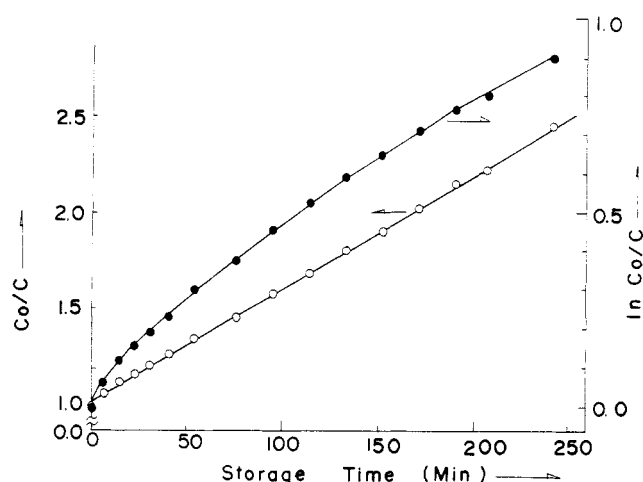


**Figure 9.** Inverse concentration ( $C_0/C$ ) and logarithm of inverse concentration ( $\ln C_0/C$ ) of anilino radicals versus storage time at 117 °C. The values of  $C_0/C$  and  $\ln C_0/C$  were calculated from the data for PMMA (●) in Figure 8.

lecular compatibility of the two polymers.

**Decay of Anilino Radicals Labeled at the Chain End Sites of PMMA.** Samples of labeled polymers were annealed at 173 °C for 15 min and quenched to -196 °C. The sample tube was then inserted into the ESR cavity maintained at a reaction temperature, and ESR spectra were recorded at appropriate time intervals. The total concentrations of radicals were obtained by double integration of the first derivative patterns, and the percent concentrations of radicals were obtained as a function of annealing time. The decay curves of anilino radicals are shown in Figure 8, where zero time is the time of the first ESR measurement. The same procedure was carried out at different reaction temperatures to obtain the temperature dependence of the kinetic constant. The decay rate of the radicals increases with increasing PVDF content of the blends.

From these data, the inverse concentrations,  $C_0/C$ , and the logarithms of the relative concentration,  $\ln C_0/C$ , were plotted against storage time (Figure 9). Here  $C_0$  is the initial concentration of the radicals. As seen from Figure 9,  $\ln C_0/C$  deviates from a linear plot, but  $C_0/C$  is linear with storage time:

$$C_0/C = a + KC_0t \quad (1)$$

Therefore the decay reaction follows second-order kinetics, and the radicals decay by a bimolecular reaction that in-

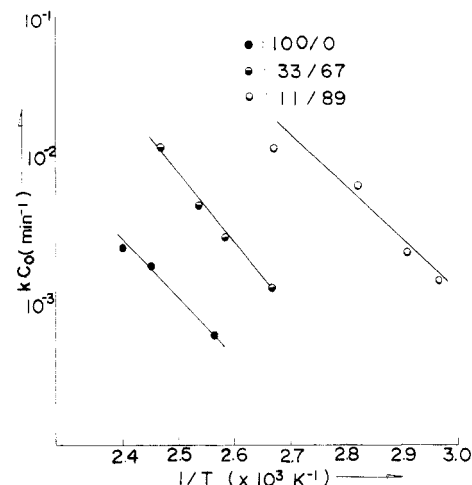


**Figure 10.** Temperature dependence of time constant,  $KC_0$  (see text): PMMA (●), PMMA/PVDF (33/67) blend (◐) and PMMA/PVDF (11/89) blend (○).

volves translational diffusion of the chain end sites of the PMMA molecules:

$$-dC/dt = KC^2 \quad (2)$$



To analyze the diffusion-controlled bimolecular reaction, we<sup>10</sup> modified Waite's equation<sup>11,12</sup> as follows:

$$C_0/C = 1 + At^{1/2} + Bt \quad (4)$$

$$A = 8(2^{1/2}r_0^2C_0)(\pi D)^{1/2} \quad (5)$$

$$B = 8\pi r_0 D C_0 \quad (6)$$

where  $r_0$  is the capture radius and  $D$  is the diffusion constant. When the experimental condition is  $t \gg (A/B)^2$ , eq 4 coincides with eq 1. From eq 1, 4, and 6, the kinetic constant  $K$  is found to be proportional to the diffusion constant of the radicals:

$$K = 8\pi r_0 D \quad (7)$$

The temperature dependence of the time constant  $KC_0$  in eq 1 is shown in Figure 10. The constants at 375 K in the blends 33/67 and 11/89 are 6 and 90 times, respectively, larger than that in PMMA.

When PMMA chains are dilute in PVDF matrices, the value of  $C_0$  decreases with increasing PVDF content when PMMA and PVDF are compatible. The time constant  $KC_0$  increases with PVDF content despite the decrease in  $C_0$ . From eq 7, the constant of translational diffusion of radicals also increases with PVDF content. The translational diffusion of the PMMA chain in the blend should reflect the molecular compatibility of PMMA and PVDF chains in the blends, and the PVDF chains should have a plasticizing effect on the PMMA chains. Thus the excess free volume introduced by the addition of diluent PVDF chains should cause an increase in the rates of rotational and translation molecular motions.

**Registry No.** PVDF, 24937-79-9; PMMA, 9011-14-7; 2,4,6-tri-*tert*-butylnitrosobenzene, 24973-59-9.

## References and Notes

- (a) Nishi, T.; Wang, T. T. *Macromolecules* **1975**, *8*, 909. (b) Hirata, Y.; Kotaka, T. *Polym. J.* **1981**, *13*, 273. (c) Wendorff, J. H. J. *Polym. Sci., Polym. Lett. Ed.* **1980**, *18*, 439. (d) Bliznyuk, V. N.; Shilov, V. V.; Gornza, Yu. P.; Lipatov, Yu. S. *Polym. Sci. USSR* **1985**, *77*, 147. (e) Hahn, B.; Wendorff, J.; Yoon, D. Y. *Macromolecules* **1985**, *18*, 718. (f) Pathmanathan, K.; Johari, G. P.; Faivre, J. P.; Monnerie, L. *J. Polym. Sci.*

- Polym. Phys. Ed.* 1986, 24, 1587. (g) Hahn, B.; Wendorff, J. *Polymer* 1985, 26, 1619. (h) Saito, H.; Fujita, Y.; Inoue, T. *Polym. J.* 1987, 19, 405.
- (2) Shimada, S.; Hori, Y.; Kashiwabara, H. *Macromolecules* 1985, 18, 170 and references therein.
- (3) Kitahara, T.; Shimada, S.; Kashiwabara, H. *Polymer* 1980, 21, 1299.
- (4) Shimada, S.; Kitahara, T.; Kashiwabara, H. *Polymer* 1980, 21, 1304.
- (5) (a) Hirata, T.; Kashiwagi, T.; Brown, J. E. *Macromolecules* 1985, 18, 1410. (b) Calahorra, E.; Cortazar, M.; Guzman, G. M. *J. Polym. Sci., Polym. Lett. Ed.* 1985, 23, 257. (c) Kashiwagi, T.; Inaba, A.; Brown, J. E.; Hatada, K.; Kitayama, T.; Masuda, E. *Macromolecules* 1986, 19, 2160.
- (6) Terabe, S.; Konaka, R. *J. Am. Chem. Soc.* 1971, 93, 4306.
- (7) Murakami, K.; Sohma, J. *Polym. J.* 1979, 11, 545.
- (8) Tsay, F.; Hong, S. D.; Moacanin, J.; Gupta, A. *J. Polym. Sci., Polym. Phys. Ed.* 1982, 20, 763.
- (9) Brown, I. M.; Sandreczki, T. C. *Macromolecules* 1985, 18, 2702.
- (10) Shimada, S.; Hori, Y.; Kashiwabara, H. *Polymer* 1977, 18, 25.
- (11) Waite, T. R. *J. Chem. Phys.* 1960, 32, 21.
- (12) Waite, T. R. *Phys. Rev.* 1957, 107, 463.

## Thermodynamic and Kinetic Factors in Adsorption of Polymers on a Plane Lattice

E. Pefferkorn,\* A. Haouam, and R. Varoqui

Institut Charles Sadron, CNRS (CRM-EAHP), 6 Rue Boussingault, 67083 Strasbourg Cedex, France. Received October 26, 1987

**ABSTRACT:** The rate of formation of an adsorbed polystyrene monolayer onto silica/carbon tetrachloride interfaces is studied by a radioactive tracer method with  $^3\text{H}$ -labeled polymers. The influence of the temperature on the amount of the polymer adsorbed is determined, and the kinetic law of the adsorption is formulated. At low solution concentrations, the polymer adsorbs with a very flattened conformation, and the kinetic parameter of the adsorption process is quantitatively analyzed with use of a mechanism corresponding to a two-dimensional lattice filling. This process may be regarded as a "solution" process such as the mixing on a molecular scale, which involves, beside surface forces, local conformational changes and entropy of mixing effects. At higher solution concentrations, loops and/or tails emerge from the surface at a very low rate.

### Introduction

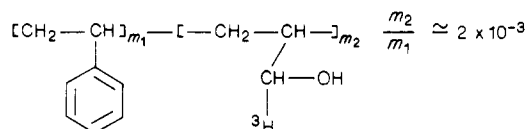
Several studies of the adsorption of polystyrene onto silica, carbon, and metal surfaces under various solvent conditions have been reported in the literature.<sup>1-8</sup> Several characteristics of the polymer layer adsorbed on these substrates were determined: macromolecular interfacial area, hydrodynamic and ellipsometric thicknesses, and relative importance of trains and loops at adsorption equilibrium. Special interest was also directed toward the variation of the number of chain segments in contact with the solid surface, resulting from the increase in the degree of coverage. These adsorption studies were done on plane, porous, or finely divided adsorbents, suited to the selected techniques of investigation.<sup>9</sup>

In the present study, we focused attention on the kinetics of the formation of a polymer layer on a nonporous silica adsorbent of particular interest. By choosing an adsorbent, fully hydrated silica, bearing only silanol groups and carbon tetrachloride as solvent, we were able to generate strong polymer-surface interaction forces and to follow the early stages corresponding to the formation of a flat carpet.<sup>10</sup> Information relative to the layer structure and to the successive conformations of the adsorbed polymer was obtained by varying the polymer concentration in the solution at adsorption equilibrium. Similarly the influence of temperature on the shape of the adsorption isotherms furnished a scheme complementary to the observed unusually stable structure of the adsorbed polymer. It then proved interesting to establish the relationship for the kinetics of the establishment of the adsorbed layer and therefore to determine the main mechanism of the process.

### Experimental Section

**Materials. Polymer.** The radiolabeled polystyrene was prepared by radical polymerization in the presence of traces of acrolein. After purification, the polymer was reacted in freshly

distilled dioxane with tritiated potassium borohydride to yield the following chemical structure:



The characteristics of the polymer are as follow:  $M_w = 3.6 \times 10^5$ ,  $M_w/M_n$  (GPC) = 1.6; specific radioactivity  $R_s = 2 \times 10^8$  cpm  $\text{g}^{-1}$ . The polymer concentration was obtained by determining the specific radioactivity of the solution. Because the carbon tetrachloride exerts a strong quenching, the solvent was extracted before the liquid scintillator (Instagel Packard) was added to the polymer sample.

**Adsorbent.** The adsorbent was nonporous glass beads (Verre et Ind.) of 34- $\mu\text{m}$  average diameter and  $7.8 \times 10^{-2} \text{ m}^2 \text{ g}^{-1}$  specific surface area. This adsorbent was treated with hot hydrochloric acid to extract or exchange with  $\text{H}^+$  all surface ionic exchangeable species. Moreover, this treatment generates a hydrated silanol surface. The beads were then washed free of acid. Excess water was evaporated under reduced pressure at 40  $^\circ\text{C}$ . This soft drying process maintains the fully hydrated silanol surface.<sup>11</sup>

**Solvent.** Carbon tetrachloride was dried over  $\text{CaH}_2$ , distilled under  $\text{N}_2$ , and maintained over molecular sieves. The polystyrene solutions were kept at the selected temperature for 5 days before use in adsorption experiments to reach conformational equilibrium.

**Procedures. Adsorption Isotherms.** Silica beads were suspended in the solvent and degassed under reduced pressure to generate the true solid-liquid interface. The required mass of polymer solution was then added to the suspension. Great care was taken to isolate the suspension from atmospheric moisture. Mild controlled agitation was used to renew the sediment/supernatant interface. The amount of adsorbed polymer was determined by counting the radioactivity of the supernatant solution. This was done at different time intervals, and the actual adsorption was calculated when no systematic variation could be detected over 3 days.

**Adsorption Rate Determination.** Glass beads (1 g) and approximately 20 mL of carbon tetrachloride were introduced into